Bounds on the attractor dimension for low-R_m wall-bound magnetohydrodynamic turbulence

Cite as: Phys. Fluids **18**, 125102 (2006); https://doi.org/10.1063/1.2391841
Submitted: 03 May 2006 • Accepted: 13 October 2006 • Published Online: 04 December 2006

Alban Pothérat and Thierry Alboussière

Bounds on the attractor dimension for low-R_m wall-bound magnetohydrodynamic turbulence

Alban Pothérat[a)]
Ilmenau Technical University, Kirchoffstrasse 1, 98693 Ilmenau, Germany

Thierry Alboussière[b)]
Laboratoire de Géophysique Interne et Tectonophysique, CNRS, Observatoire de Grenoble, Université Joseph Fourier Maison des Géosciences, BP 53, 38041 Grenoble Cedex 9, France

(Received 3 May 2006; accepted 13 October 2006; published online 4 December 2006)

Steady low-R_m magnetohydrodynamic (MHD) turbulence is investigated here through estimates of upper bounds for attractor dimension. A flow between two parallel walls with an imposed perpendicular magnetic field is considered. The flow is defined by its maximum velocity and the intensity of the magnetic field. Given the corresponding Reynolds and Hartmann numbers, one can rigorously derive an upper bound for the dimension of the attractor and find out which modes must be chosen to achieve this bound. The properties of these modes yield quantities that we compare to known heuristic estimates for the size of the smallest turbulent vortices and the degree of anisotropy of the turbulence. Our upper bound derivation is based on known bounds of the nonlinear inertial term, while low-R_m Lorentz forces—being linear—can be relatively easily dealt with. The simple configuration considered in this paper allows us to identify some boundaries separating different sets of modes in the space of nondimensional parameters, which are reminiscent of three important previously identified transitions observed in the real flow. The first boundary separates classical hydrodynamic sets of modes from MHD sets where anisotropy takes the form of a "Joule cone." In the second, one can define the boundary separating three-dimensional (3D) MHD sets from quasi-two-dimensional (2D) MHD sets, when all "Orr-Sommerfeld modes" disappear and only "Squire modes" are left. The third separates sets where all the modes exhibit the same boundary layer thickness or so, and sets where many different "boundary layer modes" coexists in the set. The nondimensional relations defining these boundaries are then compared to the heuristics known for the transition between isotropic and anisotropic MHD turbulence, 3D and quasi-2D MHD turbulence, and that between a turbulent and a laminar Hartmann layer. In addition to this 3D approach, we also determine upper bounds for the dimension of forced turbulent flows modeled using a 2D MHD equation, which should become physically relevant in the quasi-2D MHD regime. The advantage of this 2D approach is that, while upper bounds are quite loose in three dimensions, optimal upper bounds exist for the 2D nonlinear term. This allows us to derive realistic attractor dimensions for quasi-2D MHD flows. © *2006 American Institute of Physics*.
[DOI: 10.1063/1.2391841]

I. INTRODUCTION

Magnetohydrodynamic (MHD) turbulence at low magnetic Reynolds number is relevant to many laboratory-scale experiments[1–4] as well as to many industrial processes.[5,6] This is a consequence of the small values of liquid metal Prandtl numbers Pm, around 10^{-6}. With magnetic fields in the range $0.1-1$ T, length scales $0.1-1$ m and flow velocities of $0.01-1$ m/s, it is likely that Lorentz forces will have a great impact on liquid metal flow turbulence and unlikely that the flow will affect the imposed magnetic field, as magnetic diffusivity exceeds kinematic viscosity by a factor $Pm^{-1}=10^6$. Unexpectedly, MHD turbulence can also be relevant to large magnetic Reynolds numbers when the magnetic Prandtl number is small. This is the case for the geodynamo, for which the magnetic Prandtl number is about 10^{-6}. In this case, going from large eddies to smaller ones, the magnetic turbulent cascade stops long before the hydrodynamic cascade. The small scales of large-R_m turbulence can thus be considered as an example of low-R_m turbulence.

The question of how turbulence looks can be addressed theoretically in a number of ways, most of them based on physical assumptions or turbulence models as recently in Ref. 7. It is, however, possible to make no assumption and although this leads to limited information, this is reliable information on which further studies can be based, for instance the derivation of a turbulence model. In this paper, we have estimated upper bounds for the attractor dimension of low-R_m MHD turbulent flows, a quantity that can be rigorously linked to the size of the dissipative scales[8] and therefore provides some crucial information on the flow. Our work is based on previous non-MHD studies of Navier-Stokes attractors in three and two dimensions. It has been shown that the attractor of turbulent solutions is of finite

[a)]Electronic mail: alban.potherat@tu-ilmenau.de
[b)]Electronic mail: talbouss@obs.ujf-grenoble.fr

dimension even though the set of possible functions is of infinite dimension. This is basically due to viscous effects setting a maximum curvature to possible solutions. In three dimensions (3D), the fundamental questions of the smoothness of solutions of Navier-Stokes equations and of the existence of a compact attractor remain open. We assume this is the case and this constitutes the only assumption. We do not need to make such assumptions for the two-dimensional (2D) case as smoothness has been proved. In addition, previous upper bounds of attractor dimensions for 2D flows coincide very nearly with heuristic estimates based on the cascade of enstrophy.[8,9] This is not the case for 3D rigorous upper bounds as they are found to be much larger than heuristic estimates based on the cascade of energy.[8,10]

Our main goal is basically to extend the non-MHD studies to the case of low-R_m MHD. As Lorentz forces are linear forces, this does not include additional theoretical difficulties. However, as these forces are strongly dissipative, the final upper bounds for attractor dimensions are significantly affected when imposing a magnetic field. Together with the upper bounds, we put in evidence the modes that achieve the upper bound for the attractor dimension. We then determine boundaries separating different sets of these modes exhibiting the same properties as real turbulent flows. These boundaries are encountered when increasing the imposed magnetic field and strongly resemble known transitions occurring in the flow. The chosen configuration of study is taken as simple as possible to enable us to show these transitions: the electrically conducting fluid is contained between two parallel infinite walls, and a perpendicular magnetic field is applied. The flow is held steady on average by application of a forcing that is independent of the velocity field. First, it is expected that isotropic turbulence becomes anisotropic by stretching in the direction of the magnetic field.[11] Second, the turbulent Hartmann boundary layers which develop along the walls become laminar and thirdly, a quasi-2D regime is obtained.

Three similar boundaries between sets of modes can be observed and determined formally by analyzing rigorous upper bounds for attractor dimension and the corresponding set of vector-valued functions. The first one is defined by the absence of functions with variations along the magnetic field direction outside (Hartmann) boundary layers and with no variation in the perpendicular directions. The third boundary is found when this absence is independent of any condition regarding perpendicular variations. Finally, the second boundary corresponds to the presence modes with other length scales close to the walls than the laminar Hartmann layer thickness.

The method of estimates of dimension upper bounds for attractors is presented in Sec. II. Section III is devoted to the determination of least dissipative modes. In Secs. IV and V we determine the attractor dimension of 3D and 2D turbulent flows, respectively, discuss the various boundaries found, and compare them to the transitions observed as the nature of turbulence changes with the intensity of the magnetic field. Comments on this work and results are presented in Sec. VI, where the relevance of the least dissipative modes to the real flow is discussed.

II. METHOD TO DETERMINE THE ATTRACTOR DIMENSION

From the point of view of dynamical systems, the phase space of turbulence is the infinite-dimensional set of all vector-valued functions in which Navier-Stokes solutions evolve as time goes on. If the attractor is compact, its finite dimension d can be determined using the fact that any solution to the Navier-Stokes equations should eventually become arbitrarily close to the attractor. Let us then consider an infinitesimal n-dimensional box around a solution. As time passes, each point in the box evolves according to the Navier-Stokes equations. Eventually, this box will then end up within the attractor. This provides a criterion on the fate of the volume of the box: if $n>d$, the volume of the box will converge towards zero, in the same way as a cube has to have a vanishing volume if it is to fit in a surface of zero thickness. As soon as $n<d$, the volume of the box will not converge towards zero, i.e., it will either not converge, converge towards a finite value, or diverge—should ergodicity hold—as the box spreads into the whole attractor.

The evolution of the size of n-dimensional infinitesimal boxes is intimately related to the Lyapunov exponents. The nth Lyapunov exponent is the maximal rate of growth of the nth dimensional volume spanned by n infinitesimal disturbances about a solution at large time (i.e., in the attractor). Denoting $\mathcal{A}$ the linearized Navier-Stokes equations, a disturbance $\delta\mathbf{u}$ about a solution $\mathbf{u}$ obeys the following equation:

$$\frac{\partial}{\partial t}\delta\mathbf{u} = \mathcal{A}(\mathbf{u})\,\delta\mathbf{u} + \mathcal{O}(\delta\mathbf{u}^2). \tag{1}$$

Considering n orthonormal disturbances spanning a n-volume $V_n = \|\delta\mathbf{u}_1 \times \cdots \times \delta\mathbf{u}_n\|$, the equation for a single disturbance (1) can be generalized and integrated to provide an expression for V_n (see Ref. 12):

$$V_n(t) = V_n(0)\exp(t\langle \mathrm{Tr}[\mathcal{A}P_n]\rangle), \tag{2}$$

where P_n denotes the projection onto the n-dimensional subspace spanned by the n disturbances at initial time, and the bracket $\langle\,\rangle$ stands for a long time average. For each integer value n, we determine the n largest eigenvalues of $\mathcal{A}$ and consider whether their sum is larger or smaller than zero. In the first case, n is smaller than the attractor dimension, and in the second case, n is larger than the attractor dimension.

Nonlinear terms can stretch solutions and are pushing eigenvalues towards positive values, while dissipative terms make solutions shrink (in phase space) and lead to negative eigenvalues. The largest eigenvalues are obtained for large scale functions while small scales vector fields produce more dissipation and thus negative eigenvalues. Hence, large scale motions are selected first to calculate the first Lyapunov exponents. Their number is limited though and eventually one has to select negative eigenvalues. Eventually, when enough negative values are added up, they balance the initial positive eigenvalues and Lyapunov exponents themselves become negative. The nth Lyapunov exponent for which this happens roughly yields the dimension of the turbulent attractor. (These dimensions are numbers much larger than 1, so we do not need to worry very long about their exact noninteger

value between $n-1$ and n. For low-dimensional attractors, the Kaplan-Yorke formula can be used to determine this value precisely.[13])

The above cross products and projection require the existence of a scalar product in the phase space of vector valued functions (in 2D or 3D space). In this study we shall use the standard L^2 Hilbert structure. Given $\mathbf{u}$ and $\mathbf{v}$, two vector fields, their scalar product is defined as

$$\mathbf{u}\cdot\mathbf{v}=\int_{\mathcal{V}} u_i v_i^* dV, \tag{3}$$

where $i=1,2$ or $i=1,2,3$ for 2D or 3D turbulence. We are considering here low R_m turbulence under the condition of diffusive magnetic field, i.e., the quasi-static model of MHD. If one considers a small perturbation, $\delta\mathbf{u}$, its evolution is thus governed by the following equations:

$$\partial_t\delta\mathbf{u}=-\nabla\delta p-\mathbf{u}\cdot\nabla\delta\mathbf{u}-\delta\mathbf{u}\cdot\nabla\mathbf{u}+\nu\left(\nabla^2+\frac{\sigma B^2}{\rho\nu}\nabla^{-2}\partial_{zz}^2\right)\delta\mathbf{u}, \tag{4}$$

$$\nabla\cdot\delta\mathbf{u}=0, \tag{5}$$

with associated boundary conditions for the perturbation:

$$\forall\mathbf{x}\in\mathbb{R}^3,\ \forall\, k_x,k_y\in\mathbb{Z},\quad \mathbf{v}(\mathbf{x})=\mathbf{v}(\mathbf{x}+k_xL\mathbf{e}_x)=\mathbf{v}(\mathbf{x}+k_yL\mathbf{e}_y), \tag{6}$$

$$\mathbf{v}(z=-L)=\mathbf{v}(z=L)=0, \tag{7}$$

where σ, ρ, and ν are the fluid's electric conductivity, density, and kinematic viscosity, respectively. B is the intensity of the magnetic field, which points in the z direction. The perturbation in electric current $\delta\mathbf{j}$ is related to $\delta\mathbf{u}$ by

$$\delta\mathbf{j}=-\sigma B\nabla^{-2}\partial_z\nabla\times\delta\mathbf{u} \tag{8}$$

and must satisfy the perturbed form of the electric current conservation $\nabla\cdot\delta\mathbf{j}=0$ as well as the condition that the walls located at $z=-L$ and $z=L$ are electrically insulating:

$$\delta j_n=0, \tag{9}$$

where δj_n is the component of $\delta\mathbf{j}$, which is normal to the wall.

The trace of the evolution operator is split into nonlinear and linear parts, $\mathcal{A}(\mathbf{u})\delta\mathbf{u}=\mathcal{B}(\mathbf{u},\delta\mathbf{u})+\mathcal{L}(\delta\mathbf{u})$. For any disturbance $\delta\mathbf{u}$ of norm unity, the contribution of the nonlinear term to the trace operator is expressed as

$$\int_{\mathcal{V}}\delta\mathbf{u}\cdot\mathcal{B}(\mathbf{u},\delta\mathbf{u})dV=\int_{\mathcal{V}}\delta\mathbf{u}\cdot[-\nabla\delta p-\mathbf{u}\cdot\nabla\delta\mathbf{u}-\delta\mathbf{u}\cdot\nabla\mathbf{u}]dV. \tag{10}$$

It has been shown in Ref. 14 that this contribution can be bound as follows:

$$\int_{\mathcal{V}}\delta\mathbf{u}\cdot\mathcal{B}(\mathbf{u},\delta\mathbf{u})dV\le|\nabla\delta\mathbf{u}|_{L^2}|\mathbf{u}|_{L^\infty}\le-\frac{\nu}{2}\int_{\mathcal{V}}(\nabla^2\delta\mathbf{u})\cdot\delta\mathbf{u}dV+\frac{1}{2\nu}|\mathbf{u}|_{L^\infty}^2. \tag{11}$$

The first term is equal to half the viscous dissipation term with the opposite sign and the second term depends on the maximum velocity, which we assumed to be bounded. When considering n disturbances ($\delta\mathbf{u}_i$) the trace of the linearized operator $\mathcal{A}$ on the subspace spanned by these disturbances can be expressed as

$$\mathrm{Tr}(\mathcal{A}P_n)=\mathrm{Tr}(\mathcal{B}P_n)+\mathrm{Tr}(\mathcal{L}P_n)\le\frac{\nu}{2}\mathrm{Tr}(\nabla^2P_n)+\frac{\sigma B^2}{\rho}\mathrm{Tr}(\nabla^{-2}\partial_{zz}^2P_n)+\frac{n}{2\nu}|\mathbf{u}|_{L^\infty}^2. \tag{12}$$

This can be written in dimensionless terms using L for distance, U_∞ the maximum velocity for velocity, σBU_∞ for electric current density, and ν/L^3 for traces of operators:

$$\mathrm{Tr}(\mathcal{A}P_n)\le\mathrm{Tr}\left(\left[\frac{1}{2}\nabla^2+Ha^2\nabla^{-2}\partial_{zz}^2\right]P_n\right)+\frac{n}{2}Re^2, \tag{13}$$

where the Hartmann and Reynolds numbers are defined as $Ha=\sqrt{\sigma/(\rho\nu)}BL$ and $Re=U_\infty L/\nu$. This bound can be determined provided the trace of the operator $\mathcal{D}_{Ha}=1/2\nabla^2+Ha\,\nabla^{-2}\partial_{zz}$, which is nearly equal to the dissipative operator (viscous and Joule dissipation), can be evaluated. This is the subject of the next section. Before we move on to this task, it is important to notice that although the equations for $\delta\mathbf{u}$ have been linearized around an unspecified solution $\mathbf{u}$, the attractor to which $\mathbf{u}$ belongs is indeed that of the full nonlinear Navier-Stokes equations, and so is its dimension d_M.

III. LEAST DISSIPATIVE MODES IN A FLOW BETWEEN TWO HARTMANN WALLS

In the expression for the trace of the linearized evolution operator (13), the last term is positive and depends only on the number of modes n and not on which modes are considered. The other term is the trace of a linear operator, consisting of half the viscous effect and of the entire Lorentz force. This term is negative and depends on the modes selected. In order to find an upper bound for the attractor dimension, we want to select the least dissipative terms so as to get as many of them as possible before the trace vanishes. Finding the least dissipative modes boils down to an eigenvalue problem.

A. Eigenvalue problem

In this section, we solve the eigenvalue problem for the dissipation operator $\mathcal{D}_{Ha}$ in a closed box with L-periodic boundary conditions in the x and y directions and impermeable and electrically insulating walls located at $z=-L$ and $z=L$. For these boundary conditions, the Laplacian operator is invertible so that the eigenvalue problem for the $\mathcal{D}_{Ha}$ operator can be formulated using nondimensional variables as

$$(\nabla^4-2\,Ha^2\partial_{zz}^2)\mathbf{v}=2\lambda\nabla^2\mathbf{v}, \tag{14}$$

$$\nabla \cdot \mathbf{v} = 0. \tag{15}$$

Here lengths are normalized by L, velocities by an unspecified typical velocity U, the eigenvalues λ by ν/L^2, and electric currents by σBU. The choice of U is not important since the problem is linear. $\mathbf{v}$ also has to satisfy the same kinematic boundary conditions (6) and (7) as $\delta\mathbf{u}$. As in (8), an electric current field $\mathbf{J}$ is associated to $\mathbf{v}$ by

$$\mathbf{J} = -\nabla^{-2}\partial_z \Omega, \tag{16}$$

where $\Omega = \nabla \times \mathbf{v} \cdot \mathbf{J}$ must be solenoidal and satisfy the same electric boundary conditions (9) as $\delta\mathbf{j}$ at the walls located at $z=-1$ and $z=1$.

Since $\frac{\partial}{\partial x}$, $\frac{\partial}{\partial y}$, and $\frac{\partial}{\partial z}$ commute with $\mathcal{D}_{Ha}$, each component v_x, v_y, and v_z of the solution $\mathbf{v}=(v_i)_{i\in\{x,y,z\}}$ of (14) is of the form

$$v_i(\mathbf{x}) = V_i \exp(i\mathbf{k}_\perp \cdot \mathbf{x}_\perp + \phi_i)\, Z_i(z), \tag{17}$$

with $\phi_i \in]-\pi, \pi]$ and $\mathbf{k}_\perp = k_x\mathbf{e}_x + k_y\mathbf{e}_y$. The periodic boundary conditions in the x and y directions impose $(k_x, k_y) \in 2\pi\mathbb{Z}^2$. $Z_i(z) = \Sigma_j A_i^{(j)} \exp(K^{(j)}z)$, where $K^{(j)}$ are the complex roots of the dispersion equation obtained by inserting (17) into (14):

$$2\lambda = -(k_x^2 + k_y^2 + K^2) - 2\,Ha^2 \frac{K^2}{k_x^2 + k_y^2 + K^2}. \tag{18}$$

There are always two real and two imaginary roots for K: $1/\delta$, $-1/\delta$, $i\kappa_z$, and $-i\kappa_z$ with

$$-\kappa_z^2 = Ha^2 + \lambda + k_\perp^2 - \sqrt{(Ha^2+\lambda)^2 + 2k_\perp^2\, Ha^2}, \tag{19}$$

$$\frac{1}{\delta^2} = Ha^2 + \lambda + k_\perp^2 + \sqrt{(Ha^2+\lambda)^2 + 2k_\perp^2\, Ha^2}. \tag{20}$$

Eventually, each function $Z_i(z)$ is of the general form

$$Z_i(z) = A_i^1 \exp(z/\delta) + A_i^2 \exp(-z/\delta) + A_i^3 \exp(i\kappa_z z) + A_i^4 \exp(-i\kappa_z z). \tag{21}$$

Since the operator $\mathcal{D}_{Ha}$ has homogeneous boundary conditions, there is a discrete spectrum of possible values of δ and κ_z, which is determined by the boundary conditions. We shall now express the boundary conditions for the Z_i functions derived in the previous section. The impermeability conditions at $z=-1$ and $z=1$ yield readily

$$Z_i(-1) = 0, \tag{22}$$

$$Z_i(1) = 0, \tag{23}$$

which, by virtue of the continuity equation (15) implies

$$Z_z'(-1) = 0, \tag{24}$$

$$Z_z'(1) = 0. \tag{25}$$

Using (16) to calculate $J_z(z=-1)$ and $J_z(z=1)$, then using the dispersion equation (18), the electric conditions at the walls located at $z=-1$ and $z=1$ are, respectively, written as

$$-k_x\left(Z_y'(-1) - (k_\perp^2 + 2\lambda)\int Z_y(-1)\right) + k_y\left(Z_x'(-1) - (k_\perp^2 + 2\lambda)\int Z_x(-1)\right) = 0, \tag{26}$$

$$-k_x\left(Z_y'(1) - (k_\perp^2 + 2\lambda)\int Z_y(1)\right) + k_y\left(Z_x'(1) - (k_\perp^2 - 2\lambda)\int Z_x(1)\right) = 0, \tag{27}$$

where $\int Z_i(z) = \delta a_i \exp(z/\delta) - \delta b_i \exp(-z/\delta) - ic_i/\kappa_z \exp(i\kappa_z z) + id_i/\kappa_z \exp(-i\kappa_z z)$.

B. Squire and Orr-Sommerfeld modes

We shall now use the boundary conditions (22)–(27) to find the sequences of values of δ, κ_z, λ, as well as the properties of the related eigenmodes. Equations (22)–(25) impose four homogeneous conditions on the four coefficients A_z^1, A_z^2, A_z^3, and A_z^4 in the expression of Z_z. This means that the eigenmodes of the dissipation operator can be divided into two categories.

(1) For the modes of the first category, conditions (22)–(25) are redundant so that $Z_z \neq 0$. In this case, the determinant formed by those four conditions must be zero, which yields

$$4\frac{\kappa_z}{\delta} + \cosh(\kappa_z + 1/\delta)(\kappa_z - 1/\delta)^2 - \cosh(\kappa_z - 1/\delta)(\kappa_z + 1/\delta)^2 = 0. \tag{28}$$

The sequence of values of κ_z and δ is determined by writing that $-\kappa_z^2$ and δ^2 must both be roots of the dispersion equation (18) for given values of Ha, λ, k_x, and k_y. Eliminating λ between (20) and (19) yields the searched condition

$$\frac{\kappa_z^2}{\delta^2} - k_\perp^2\left(k_\perp^2 - \frac{1}{\delta^2} + \kappa_z^2 + 2\,Ha^2\right) = 0. \tag{29}$$

The system formed by (28) and (29) admits exactly one solution for (κ_z, δ) in each interval $[p\pi/2, (p+1)\pi/2] \times]0, \infty[$ with $p \in \mathbb{Z}-\{0\}$. This defines the sequence of possible values of κ_z and δ for given Ha, λ, and $k_\perp$. The related eigenmodes have a nonzero component along $\mathbf{e}_z$. By analogy with the eigenvalue problems that arise in the linear stability theory (see for instance, Ref. 15) we shall call them *Orr-Sommerfeld* modes.

(2) For the modes from the second category, conditions (26), (27), (24), and (25) are not redundant so that $Z_z=0$. The continuity equation (15) then imposes that $k_x Z_x = -k_y Z_y$ so that the eigenmodes of this category are only determined by the four coefficients A_x^1, A_x^2, A_x^3, and A_x^4 (or alternately A_y^1, A_y^2, A_y^3, A_y^4). δ and κ_z are then determined using the electric conditions at the walls (22) and (23) that, together with (26) and (27), impose four homogeneous conditions on the four coefficients A_x^1, A_x^2, A_x^3, and A_x^4; the determinant formed by these conditions has to be zero for the eigenmodes not to be trivial:

$$((\kappa_z^2 - 1/\delta^2)(k_\perp^4 - \kappa_z^2/\delta^2) + 4\kappa_z^2/\delta^2)\sin(\kappa_z)\sinh(1/\delta) + 4\,Ha^2\kappa_z/\delta(\cos(\kappa_z)\cosh(1/\delta) - 1) = 0. \quad (30)$$

Here the system formed by (30) and (29) admits exactly one solution for (κ_z, δ) in each interval $[p\pi/2, (p+1)\pi/2] \times]0, \infty[$ with $p \in \mathbb{Z}$. The related eigenmodes have no velocity component along $\mathbf{e}_z$ and those with $\kappa_z < \pi/2$ exhibit only a weak dependence on z so that we may identify them as quasi-2D modes. Following our analogy with linear stability problems, we shall name the modes of this second category *Squire* modes.

These modes can be explicated by finding the three independent coefficients from A_x^1, A_x^2, A_x^3, and A_x^4. This is done by solving the system formed by (22)–(25), which is at most of rank 3. Z_y is obtained by $k_y Z_y = -k_x Z_x$ and $Z_z = 0$. The associated eigenspace has therefore a dimension between 1 and 3.

In summary, for a given value of *Ha*, the eigenvalues $\lambda(k_\perp, \kappa_z)$ of the operator $\mathcal{D}_{Ha}$ are given by the dispersion equation (29). For a fixed value of $k_\perp$, κ_z takes one value in $]0, \pi/2[$ and two values in each interval $]p\pi/2, (p+1)\pi/2[$ with $p \in \mathbb{Z} - \{0\}$. This defines a discrete sequence of values for λ, which once sorted by increasing module yields the sequence of the least dissipative eigenmodes of the dissipation operator $\mathcal{D}_{Ha}$. At this point, the eigenmodes of the dissipation operator already exhibit a quite remarkable similarity with the known properties of a flow between two parallel plates as each of those modes exhibits "core" velocity fluctuations of wavelength (k_x, k_y, κ_z) as well as exponential boundary layers of thickness δ along the walls at $z = -1$ and $z = 1$.

C. Numerical method

By sorting the values of $\lambda(k_\perp, \kappa_z)$, we are now able to find the minimum of $|\langle \mathrm{Tr}\, \mathcal{D}_{Ha} P_n \rangle|$ for any given value of n. We shall now perform this task numerically since the values of κ_z cannot be found analytically. An upper bound for the attractor dimension as a function of *Ha* and *Re* then follows immediately. The numerical method is the same as the one already used in the case of a box with 2π-periodic boundary conditions in the three directions of space:[16] it consists of sweeping the $(k_\perp, \kappa_z)$ plane with the isodissipation (iso-λ) curves, starting at $|\lambda| = 0$. For each value of λ, we count the number of $(k_\perp, \kappa_z)$ points enclosed in the corresponding iso-λ curve and calculate the sum of λ over all of those points. Each point corresponds to an eigenvalue and should therefore be weighed by its multiplicity both when counting those points and building this sum. However, it is simpler to build the sum by taking all multiplicities equal to 1. The obtained sum for a given value of n is a slightly looser lower bound for $|\langle \mathrm{Tr}\, \mathcal{D}_{Ha} P_n \rangle|$, but this may only affect the numerical constants appearing in the final results, and not the dependence on *Ha*, *n*, and *Re*.

The difference between the present case with walls at $z = -1$ and $z = 1$ and the periodic case is that the sequence of real values of κ_z replaces that of k_z in the periodic case, which has integer values. It is important to notice that the only imprecision brought by the numerical process is that of the truncation on the sequence of numerical values of κ_z and λ, as well as that which results from the resolution of the systems of equations {(28),(29)} and {(30),(29)} using the Newton method. However, since each solution of the system is bracketed, there is no risk of finding any spurious eigenvalues. In this sense, the method can be considered to give an exact result. It should also be pointed out that contrarily to the periodic case where k_z has integer values, finding the sequence of values of κ_z requires high precision arithmetics since the numbers involved in (28)–(30) are very high, whereas the values of κ_z are not. Using the LONG DOUBLE type in C language allows us to reach values of *Ha* up to 5000 and 10^5 modes. Computing the sequence of minimal modes for higher values of *Ha* and *n* would require the use of multiprecision libraries.

For given values of *n* and *Ha*, the numerical algorithm yields directly the minimum of $|\langle \mathcal{D}_{Ha} P_n \rangle|$, as well as $k_{\perp_m}$, κ_{z_m}, $\delta_{\min}$, $\delta_{\max}$, which are, respectively, the maximum values of $k_\perp$, κ_z, δ, and the minimum value of δ over the set *n* least dissipative modes. The value of *n* for which the trace of the total evolution operator is zero (i.e., $\langle \mathrm{Tr}((-\mathcal{D}_{Ha} + \mathcal{B}(., \mathbf{u}))P_n) \rangle = 0$) is an upper bound for the attractor dimension. Knowing the minimum of $|\langle \mathcal{D}_{Ha} P_n \rangle|$ and using (13), the value of *Re* for which *n* is an upper bound for d_M is given by $Re = \sqrt{2}|\langle \mathrm{Tr}(\mathcal{D}_{Ha} P_n) \rangle|/n$. The results are plotted on Fig. 1.

IV. DIMENSION AND MODES OF 3D MHD ATTRACTORS

A. Set of the least dissipative modes and attractor dimension

Because the function $\lambda(k_\perp, \kappa_z, Ha\sqrt{2})$ has the same expression as the function $1/2\lambda(k_\perp, k_z, Ha)$ in the case with periodic boundary conditions in the three directions of space,[16] the upper bound for the attractor dimension $d_M(Ha, Re)$ in both cases have similar behavior. As in the periodic case, the maximum values $k_{\perp_m}$ and κ_{z_m} over the set of the *n* least dissipative modes of $k_\perp$ and κ_z can be deducted from the geometrical shape from the $\lambda(k_\perp, k_z) = \lambda_m$ curve, where λ_m is associated to the most dissipative mode of the set (see Fig. 2).

Increasing progressively the values of *Ha* for a given value of *Re*, the upper bound for the attractor dimension exhibits three different behaviors that correspond to a 3D isotropic set of modes, a 3D anisotropic set, and quasi-2D set, respectively. For low values of *Ha*, d_M varies little with *Ha*, and the set of eigenmodes of the dissipation that achieve the upper bound is located in a circle centered on the origin in the $(k_\perp, \kappa_z)$ plane. If one imagines a flow represented by a combination of such modes, it would be 3D and nearly isotropic. For higher values of *Ha*, $d_M \sim Ha^{-1}$, just like in the case with periodic boundary conditions. The least dissipative modes are located within a cardioid-shaped curve, with no modes in the vicinity of the κ_z axis. A flow featuring such modes would be strongly anisotropic with vortices elongated in the z direction. The boundary between those first two types of sets of modes can be characterized by the disappearance (respectively, appearance) of the last (respectively, first) mode of the form $(k_\perp = 0, \kappa_z \neq 0)$. When no such modes exist,

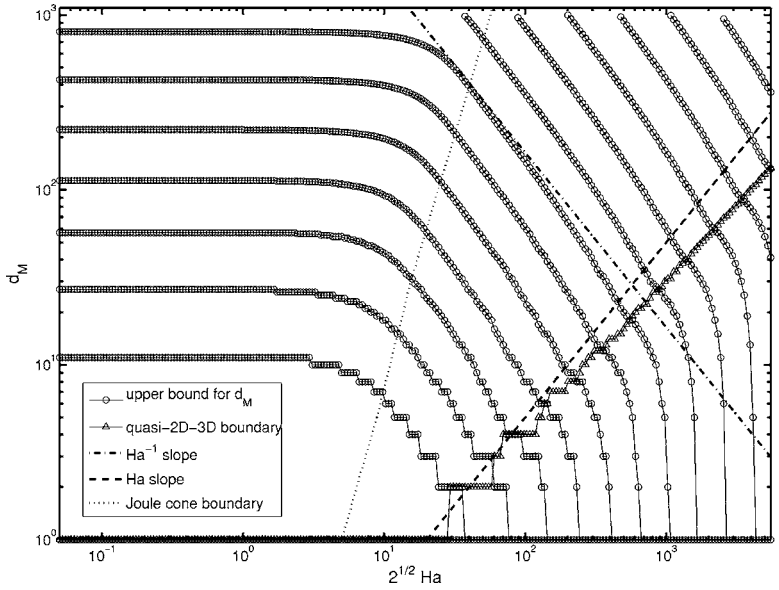

FIG. 1. Attractor dimension as a function of *Ha* for fixed values of *Re*. Three regions appear that correspond to three types of sets of modes: 3D quasi-isotropic, 3D anisotropic, and quasi-2D. Note that the attractor dimension is strongly overestimated in the quasi-2D case as the upper bound (13) applies to all flows (3D). It can be improved in the case of quasi-2D flows as shown in Sec. V.

the tangent at the origin of the iso-λ curve corresponding to the most dissipative set of eigenmodes that achieve the upper bound for d_M can be defined. All modes are then located under this line, which matches the concept of "Joule Cone" described by Ref. 17: in the existing theories of turbulence, the energy-containing modes are expelled from this cone of axis $(0,k_z)$ in the Fourier space for high values of *Ha*.

The present case with walls at $z=-1$ and $z=1$ differs from the periodic case for higher values of *Ha*, for which the related set of minimal eigenmodes of the dissipation is quasi-2D. In the periodic case, those modes all satisfy $k_z=0$ so that they are strictly 2D and produce no Joule dissipation. In this case, d_M does not vary anymore when *Ha* is increased. In the case with walls, the quasi-2D modes are Squire modes with $0<\kappa_z<\pi/2$, which exhibit an exponential velocity profile in the vicinity of the wall. This means that the associated values of $|\lambda|$ are higher in the case with walls. When the least dissipative modes are all quasi-2D Squire modes, some dissipation still arises because of the presence of the boundary layer profile at $z=1$ and $z=-1$. This results in d_M decreasing rapidly as *Ha* increases, contrarily to the periodic case. The boundary layer properties of the least dissipative modes are more specifically studied in Sec. IV D. Also, since the upper bound for the trace of the operator associated to the inertial terms (13) is a general one, which relies on no particular assumption on the flow's three- or quasi-two-dimensionality, it is unrealistic for 2D flows. An improved upper bound for the attractor dimension in the quasi-2D case is therefore derived in Sec. V, using a quasi-2D model.

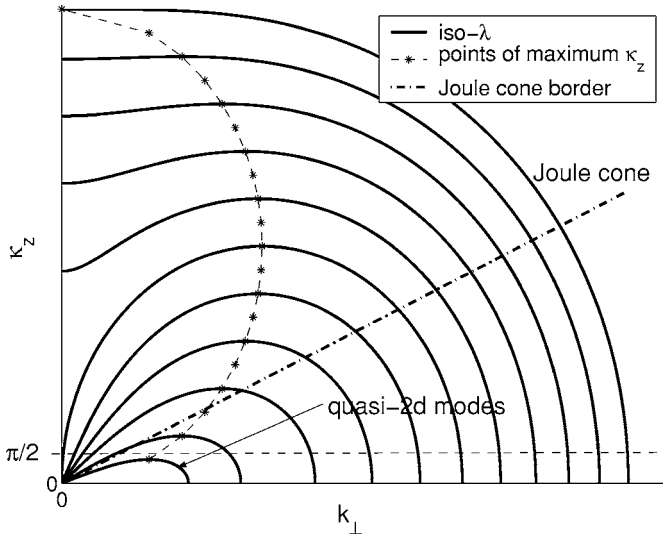

FIG. 2. Isodissipation curves in the Fourier space [one point represents all the eigenmodes with the same $(k_\perp,\kappa_z)$]. Each curve encloses the set of the *n* least dissipative modes of a given *n*. The properties (anisotropy and size of the smallest scales) from any combination of modes taken within the corresponding set can be read from the shape of the iso-λ_m curve corresponding to the value of *n* relating to the considered flow.

B. Definition of the different boundaries separating classes of least dissipative modes

For a given value of *Ha*, different types of sets of least dissipative modes are encountered when *n* (or *Re*) increases. For the sake of clarity, we shall summarize here the three boundaries separating those different types of modes and their precise definitions:

- *Boundary between quasi-2D and 3D sets of modes:* Squire modes such that $\kappa_z<\pi/2$ are the least dissipative of all and represent quasi-2D velocity fields. A set of modes containing only such modes is quasi-2D. For a given value of *Ha*, the set of the least dissipative modes crosses the quasi-2D–3D boundary either when the first Orr-Sommerfeld mode or the first Squire mode with $\kappa_z>\pi/2$ appears.
- *"Joule cone" boundary*: For strong values of *Ha*, the set of least dissipative modes contains no mode located along the (O,κ_z) axis so that all modes are located outside of the Joule cone, defined by the tangent at $(k_\perp,\kappa_z)=(0,0)$ to the set of least dissipative modes (see Fig. 2). No Joule cone can therefore be defined beyond the value of *n* at which the first mode of the form $(0,0,\kappa_z)$ appears within the set. This defines what we call the *Joule cone boundary*, which separates a strongly anisotropic (with Joule cone) from a

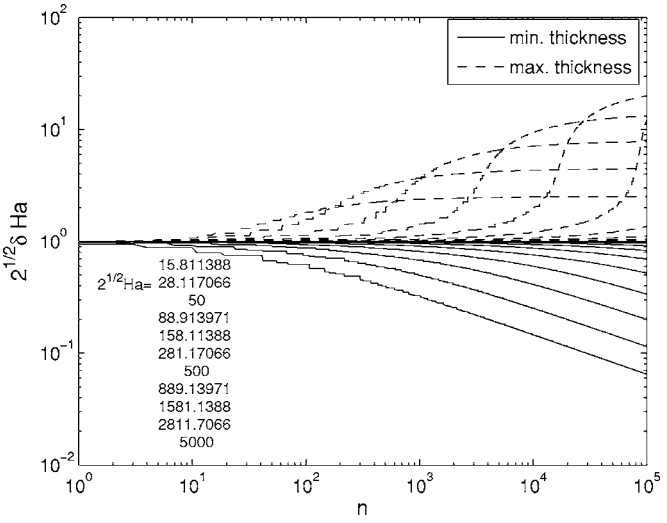

FIG. 3. Maximum and minimum of the boundary layer thickness δ over the set of modes that minimize the dissipation, as a function of n, for different values of Ha. For each Ha, a boundary appears between sets of modes where all modes have a boundary layer thickness close to $1/Ha$ (i.e., $\delta_{\min} \simeq \delta_{\max}$) and sets for which a broader spectrum of values of δ is present (i.e., $\delta_{\min} \ll \delta_{\max}$). The value of n at which this boundary is found increases with Ha.

weakly anisotropic MHD set of modes (without Joule cone).

- *Boundary between sets with single and sets with multiple boundary layer thicknesses*: The evolution of the set of values of δ, reached within the set of the least dissipative modes when n increases, exhibits a sharp transition between sets for which all values are very close to one particular value (for low n) and sets with more important scattering (larger n). The first one corresponds to a laminar boundary layer state with a well defined thickness, whereas the second exhibits strong similarities with the turbulent Hartmann boundary layer as more quantitatively explained in Sec. IV D. For a given value of Ha, we define this transition as the intersection between the line $\sqrt{2}\delta Ha=1$ and the asymptote to the curve $\delta_{\min}(n)$ when $n \to \infty$ (see Fig. 3).

When Ha is increased from 0 for a given value of n or Re, these boundaries are encountered in the reverse order. At this point it is important to underline that the properties mentioned in this section are those of the least dissipative modes and not of the real flow. The link between the two is discussed in conclusion.

C. Analytic approximation for the upper bound for d_M

We shall now derive some analytical estimates for the attractor dimension so as to be able to further compare our results to the results for the size of the dissipative scales available from Ref. 16. We consider separately either side of the Joule cone boundary defined in the previous section, i.e., 3D anisotropic sets of modes (with Joule cone) and weakly anisotropic 3D sets (without Joule cone).

As the modes are spread uniformly in the Fourier space, with $1/\pi^3$ modes per unit of volume, the value of λ_m can be found by writing that in the 1/8th space $k_x>0$, $k_y>0$, $\kappa_z>0$, the volume enclosed by the iso-λ_m curve should be $n/(8\pi^3)$. For sufficiently high values of κ_{z_m} and $k_{\perp_m}$, this can be expressed using the integrals

$$8\pi^3 \int_{V_{\lambda_m}} dk_x dk_y dk_z = n. \tag{31}$$

The trace of $\mathcal{D}_{Ha}P_n$ is similarly expressed as

$$\mathrm{Tr}(\mathcal{D}_{Ha}P_n) = 8\pi^3 \int_{V_{\lambda_m}} \lambda(k_x,k_y,k_z) dk_x dk_y dk_z. \tag{32}$$

The set of n least dissipative modes in the Fourier space is enclosed in the same iso-λ curve as the set of $8n/\pi^3$ least dissipative modes in the 2π-periodic case. The attractor dimension and the corresponding values of $k_{\perp_m}$ are then found by replacing n with $8n/\pi^3$ in the results from the study with periodic walls (Ref. 16, p. 3176). Two distinct cases are found:

(1) *Anisotropic sets of modes (with a Joule cone).* For 3D anisotropic set of least dissipative modes, all modes are located within an elongated cardioid with no mode of the form $k_\perp=0$. The Joule cone of axis $(O\kappa_z)$ exits and its half-angle it that of the tangent at the origin of the iso-λ_m curve (see Fig. 2):

$$\sin\theta_m = \sqrt{\lambda_m/Ha^2} = 2^{-1/8} 2\pi^{1/4} n^{1/4} Ha^{-3/4}. \tag{33}$$

All modes are located outside of this cone in the Fourier space. In this case, the upper bound for the attractor dimension is

$$d_M \leq \frac{9}{256\pi\sqrt{2}} \frac{Re^4}{Ha} \tag{34}$$

and the related bounds for $k_{\perp_m}$ and κ_{z_m} are

$$k_{\perp_m} \leq \left(\frac{3}{2\pi^8}\right)^{1/4} Re, \tag{35}$$

$$k_{z_m} \leq \frac{1}{\sqrt{2}} \left(\frac{3}{2\pi^8}\right)^{1/2} \frac{Re^2}{Ha}. \tag{36}$$

These sets of modes described are 3D anisotropic. For a 3D anisotropic flow, heuristic considerations of the Kolmogorov type predict $d_M \sim Re^2/Ha$, $k_{\perp_m} \sim Re^{1/2}$, and $k_{z_m} \sim Re/Ha$ (see Ref. 16).

(2) *Weakly anisotropic sets of modes (without a Joule cone).* In the case where no Joule cone can be defined within the set of dissipative mode, the related set is quasi-isotropic with

$$d_M \leq \frac{5\sqrt{30}}{216\sqrt{\pi}} Re^3 \left(1 - \frac{4\pi^3}{3}\frac{Ha^2}{Re^2}\right)^{3/2}, \tag{37}$$

and corresponding k_{z_m} and κ_{z_m}:

$$k_{\perp_m} = \sqrt{\frac{5}{\pi}} Re \left(1 - 2\pi^3 \left(\frac{2}{9} + \frac{1}{15\pi^2}\right)\frac{Ha^2}{Re^2}\right)^{1/2}, \tag{38}$$

$$\kappa_{z_m} = \sqrt{\frac{5}{\pi}}\, Re\left(1 - 2\pi^3\left(\frac{2}{9} + \frac{4}{15\pi^2}\right)\frac{Ha^2}{Re^2}\right)^{1/2}. \tag{39}$$

In the limits of small Hartmann numbers, (37) recovers the classical hydrodynamic bound for 3D turbulence of Re^3 (see, for instance, Ref. 8). The boundary between the 3D weakly anisotropic and 3D anisotropic sets of modes can be characterized by the appearance of the Joule cone. This happens when $\sin\theta_m = 1$, i.e.,

$$\frac{Ha}{Re} = \sqrt{3\pi^3}2^{5/4}. \tag{40}$$

As in the periodic case, the bounds for d_M, $k_\perp$ and κ_{z_m} exhibit the same dependence on Ha as the heuristic predictions, which suggests that our estimate renders the effect of the Lorentz force on the small scales realistically. The powers of Re are, however, overestimated, but this can be inferred to the estimate for the expansion rate of the inertial terms used in (13), which is known to be too high. The problem of finding an optimal estimate for these terms is to this day still open.

Also, one expects that when the Lorentz force becomes of the order of magnitude of inertial effects in the real flow (i.e., $Ha^2 \gtrsim Re$), the vortices start stretching in the direction of the magnetic field, so fewer of them should be present. Estimates from Kolmogorov-like arguments imply indeed that for a given Reynolds number, the number of vortices in the flow without magnetic field ($\sim Re^{3/4}$) is larger than that in a flow with strong magnetic field ($\sim Re/Ha$) as soon as $Ha \gtrsim Re^{-1/4}$. This property is recovered from the results on the upper bound for d_M since $d_M(Ha)$ clearly decreases when Ha increases at any fixed Re (see Fig. 1). (34) and (37), however, imply that this decrease starts for $Ha > Re$, which in most real cases would correspond to a laminar flow (i.e., $d_M = 0$). This is clearly unrealistic and stems again from the fact that the estimate for the trace of the inertial terms $n\,Re^2$ from which d_M is derived for both hydrodynamic and strongly anisotropic MHD flows is even further away from the heuristic estimate derived using Kolmorogov-like arguments in the MHD case ($\sim n\,Re$) than in the hydrodynamic case ($\sim n\,Re^{3/2}$).

In the two cases of 3D flow with and without the Joule cone, the upper bound for the attractor dimension exhibits the same dependence on the nondimensional numbers as in the case with periodic boundary conditions. This confirms the tendency already observed on the numerical results from the previous section. It also suggests that problems with periodic boundary conditions in the three directions of space provide some scaling laws that are relevant to cases involving more realistic boundary conditions like impermeable walls as long as the velocity field is strongly 3D. This relevance, however, breaks down for quasi-2D velocity fields, the dynamics of which is controlled by the boundary layers that arise along the walls perpendicular to the magnetic field.

D. Boundary layer properties

We now turn our attention to the influence of the walls on the modes minimizing the dissipation, as there lies the most important difference between the periodic case and the case with walls. More precisely, we shall study the values of the boundary layer thickness δ which characterizes the eigenmodes of the dissipation.

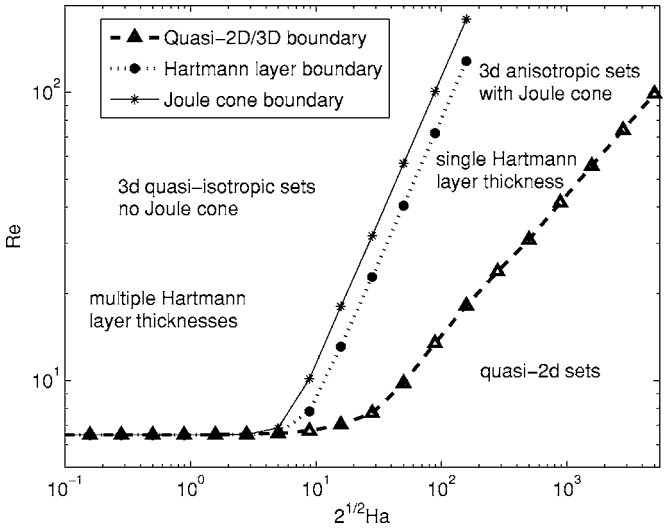

FIG. 4. Map of the different types of sets of modes in the (Ha, Re) plane.

As mentioned in Sec. III A, each mode (k_x, k_y, κ_z) can alternately be represented by the triplet (k_x, k_y, δ). Figure 3 represents the evolution of the minimum (respectively, maximum) value of δ reached within the set of the n least dissipative modes $\delta_{\min}$ (respectively, $\delta_{\max}$) as a function of n, obtained numerically from {(28), (29)} and {(30),(29)}. For each fixed value of Ha, there is an approximate value n_H of n, which marks a boundary between two types of sets of least dissipative modes: for $n < n_H$, all modes are characterized by a value of δ close to $1/Ha$ (i.e., $\delta_{\min} \simeq \delta_{\max}$) whereas for $n > n_H$, the set of least dissipative modes exhibits a much broader spectrum of values of δ (i.e., $\delta_{\min} \ll \delta_{\max}$). A velocity field represented by a combination of modes taken below this value of n would exhibit a laminar boundary layer of thickness $1/Ha$, with an exponential profile. This matches exactly the prediction of the laminar Hartmann layer theory (see, for instance, Ref. 18). For $n > n_H$, some modes appear with a thicker boundary layer, as well as modes with a layer much thinner than $1/Ha$. This two-layer structure strongly resembles that of the theoretical prediction of Ref. 19 for the turbulent Hartmann layer, which also involves such a double deck structure, with a viscous sublayer.

In order to quantify how n_H depends on the parameters Ha, n, and Re, we define it quantitatively as the value of n where the line $\sqrt{2}\delta Ha = 1$ (see Fig. 3) intersects the asymptote to the curve $\delta_{\min}(n)$ for each value of Hartmann and we have plotted the result on Fig. 4. It is remarkable that the boundary between sets of modes with a single boundary layer thickness and sets with multiple boundary layer thicknesses is never found between quasi-2D sets of modes, but always where 3D modes are present. This strong property seems to differ from the results of Ref. 20, who studied numerically the transition to turbulence of the Hartmann layer in channel flows and found that there can exist a 2D region outside of the turbulent Hartmann layer. A comparison to the

real flow in this particular instance is, however, not straightforward since even if we assume that the flow can indeed be represented by a combination of least dissipative modes, some of which are 3D, the flow can still exhibit some 2D features, as explained in conclusion.

These numerical results can be supported by some analytical expressions for the minimum and maximum boundary layer thickness, which can be obtained by eliminating $k_\perp^2$ between (19) and (20). This defines the iso-λ curves in the (δ, κ_z) plane, which enclose the set of least dissipative modes. Then remarking that the maximum and minimum values of δ are obtained for $\kappa_z=0$ yields the expressions for $\delta_{\min}$ and $\delta_{\max}$ (κ_z is never zero so these values of $\delta_{\min}$ and $\delta_{\max}$ are never reached: $\delta_{\max}$ is a close upper bound and $\delta_{\min}$ is a close lower bound):

$$\delta_{\min} = \frac{1}{\sqrt{2}} \frac{1}{\sqrt{Ha^2 - \lambda_m}}, \tag{41}$$

$$\delta_{\max} = \frac{1}{\sqrt{2}} \frac{1}{\sqrt{Ha^2 + \lambda_m}}. \tag{42}$$

In the case of a 3D set of modes with a Joule cone ($1/\sqrt{2}\, Ha \leq \lambda_m \leq Ha^2$), $\delta_{\min}$ and $\delta_{\max}$ are expressed as functions of Ha and Re using (33) and (34):

$$\delta_{\min} = \frac{1}{\sqrt{2}} \frac{1}{Ha\sqrt{1 + \frac{1}{2\pi^3}\frac{Re^2}{Ha^2}}}, \tag{43}$$

$$\delta_{\max} = \frac{1}{\sqrt{2}} \frac{1}{Ha\sqrt{1 - \frac{1}{2\pi^3}\frac{Re^2}{Ha^2}}}. \tag{44}$$

For low Reynolds numbers [or low values of $|\lambda_m|$ in (41) and (42)], $\delta_{\min}$ and $\delta_{\max}$ are very close to each other, whereas they separate quickly when Re/Ha approaches unity, as confirmed by the numerical results on Fig. 4. Remarkably, $Re/Ha \sim 1$ coincides also approximately with the disappearance of the Joule cone (40).

As for the turbulent quantities discussed in Sec. IV A, the boundary layer properties of the least dissipative modes exhibit some striking similarities with that of existing theories.[18] Quantitatively, the boundary layer thickness associated to those modes has the same dependence on Ha as that of real Hartmann layers. This adds up to the conclusion of Ref. 16, who found that the set of least dissipative modes in a 3D periodic box share many of their properties with those of the real turbulent low (Joule cone angle, small scales, boundary between quasi-2D and 3D sets of modes). Indeed, when walls are present, not only are the turbulent properties of the core flow recovered, but also some of the fine properties of the Hartmann boundary layers are closely mimicked by the least dissipative modes (thickness, boundary between sets of modes with a single boundary layer thickness of Ha^{-1}, and sets of modes with multiple thicknesses).

V. ATTRACTOR DIMENSION FOR A 2D MHD MODEL

To conclude this search for an upper bound for the attractor dimension of a turbulent MHD flow in a box with Hartmann walls, we shall now derive a tighter bound in the case where the flow is 2D by using 2D motion equations. Such equations are often used to model quasi-2D flows between two parallel insulating planes. They are obtained by averaging the full 3D Navier-Stokes equations along the direction of the magnetic field between the two planes. The model is closed by assuming a particular velocity profile along this direction. Reference 17 was the first to propose such a model, in which this particular velocity profile was derived from first order matched asymptotics using the small parameters $1/Ha$ and Re/Ha^2. At this order, the velocity profile does not vary along the direction of the magnetic field, except in the vicinity of the walls where Hartmann boundary layers of thickness $1/Ha$ develop with an exponential velocity profile. For a distance $2L$ between the Hartmann walls, the resulting model can be written as follows in dimensionless terms ($\mathbf{u}$ is normalized by ν/L):

$$\frac{\partial}{\partial t}\mathbf{u} + \mathbf{u}\cdot\nabla\mathbf{u} + \nabla p = \nabla^2\mathbf{u} - Ha\,\mathbf{u} + \mathcal{G}\mathbf{f}, \tag{45}$$

where the Hartmann number is defined as previously $Ha = \sqrt{\sigma/(\rho\nu)}BL$ and the Grashoff number is the dimensionless measure of a 2D forcing $\mathbf{f}$, defined as $\mathcal{G} = |\mathbf{f}|_{\mathcal{L}^2} L^2/\nu^2$. As in the previous sections, this forcing ensures that the flow is steady on average as the energy it injects in the flow is balanced by the dissipation (here either by viscous friction or by the linear friction term).

Even though this model is obtained at the cost of an approximation on the full 3D equations, the properties of the related dynamical system are still interesting to investigate since this model has proved its accuracy in many instances.[4,21,22] We shall now derive an upper bound for the attractor dimension d_{2D} for the related problem with L-periodic boundary conditions in the two directions of space $\mathbf{e}_x$ and $\mathbf{e}_y$.

The only difference between (45) and the 2D Navier-Stokes equation is the dissipation term, with related operator $\mathcal{D}_{2D} = \nabla^2 - Ha\,\mathcal{I}$, where $\mathcal{I}$ is the identity. Application of the method described in Sec. II yields an upper bound for the growth rate of any n-dimensional volume located in the vicinity of the attractor:

$$\langle \mathrm{Tr}\, \mathcal{A}P_n \rangle = \langle \mathrm{Tr}\, \mathcal{B}(\cdot, \mathbf{u})P_n + \mathrm{Tr}\, \mathcal{D}_{2D}P_n \rangle. \tag{46}$$

The trace of the Hartmann friction operator can be written exactly $\mathrm{Tr}(-Ha\,\mathcal{I}P_n) = -Ha\,n$. The trace of the other operators is taken from Eq. (3.19) of Ref. 23, and the trace of the global operator takes the following form:

$$\langle \mathrm{Tr}\, \mathcal{A}P_n \rangle \leq \frac{\mathrm{Tr}(\nabla^2 P_n)}{2} + cC^{4/3}(1 + \log C)^{2/3} - Ha\,n, \tag{47}$$

where $C = L^2/(4\pi^2\nu)\sup_{\mathbf{u}}\langle|\nabla^2\mathbf{u}|^2\rangle^{1/2}$ and c is a dimensionless constant of order unity. As it can be shown that $\mathrm{Tr}(\nabla^2 P_n) \leq -(8\pi^2)n^2$, the largest root of (47) provides an upper bound for the attractor dimension:

$$d_{2D} \leq -\frac{Ha}{2\pi} + \sqrt{\frac{Ha^2}{4\pi^2} + 4cC^{4/3}(1+\log C)^{2/3}}. \quad (48)$$

Since Ref. 24 has shown that the estimate for the trace of the inertial term derived for the classical 2D theory was at least log-optimal, the final bound (48) can be reasonably expected to be just as optimal.

We now need to express C in terms of the governing dimensionless numbers Ha and $\mathcal{G}$. This is done in the Appendix. For a large-scale forcing, the following relationship is derived:

$$C \leq \frac{\mathcal{G}}{2\sqrt{Ha}}. \quad (49)$$

Neglecting logarithmic corrections, Eq. (48) can then be written as

$$\frac{d_{2D}}{c'} \leq -Ha + \sqrt{Ha^2 + c''\mathcal{G}^{4/3}\,Ha^{-2/3}}, \quad (50)$$

where c' and c'' are other dimensionless constants of order unity.

Two limit cases are of interest, depending on the relative strength of $\mathcal{G}$ and Ha^2. When $\mathcal{G}$ is much larger than Ha^2, the attractor dimension can be bound as $d_{2D} \leq \mathcal{G}^{2/3}\,Ha^{-1/3}$, where constants of order unity are dropped. On the contrary, when Ha^2 is much larger than $\mathcal{G}$, an expansion of (50) leads to $d_{2D} \leq \mathcal{G}^{4/3}\,Ha^{-5/3}$.

Finally, it is possible to use this 2D result on the attractor dimension where inertial terms are probably well estimated to gain knowledge on the boundary between quasi-2D and 2D sets of modes. If we interpret d_{2D} as the number of modes present in the quasi-2D set of modes, which achieves the upper bound for d_M for a given value of Ha and $\mathcal{G}$, this quasi-2D/3D boundary obtained numerically in Sec. IV A as a function of n (number of modes) and Ha can also be expressed in terms of $\mathcal{G}$ and Ha. The result is reported on Fig. 5. Since the bound (50) can reasonably be expected to be optimal, so can be the quasi-2D/3D boundary. The curve suggest that for sufficiently large Hartmann numbers, the quasi-2D/3D boundary is approximately located at $\mathcal{G} \sim Ha^{4/5}$. This prediction has the advantage to be comparable to the transition between quasi-2D and 3D turbulence that occur in experiments as the case with walls studied here corresponds to realistic experimental conditions. Also, for a given value of Ha, the quasi-2D/3D boundary in the case with walls happens for higher values of $\mathcal{G}$ as in the periodic case ($\mathcal{G} \sim Ha^{2/3}$ from Ref. 16). This is a consequence of the extra dissipation from the Hartmann layer friction, which is absent in the periodic case.

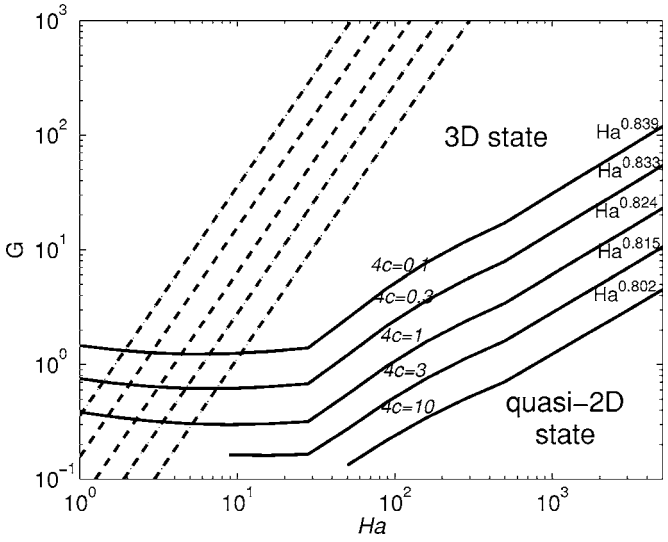

FIG. 5. Quasi-2D/3D boundary in the $\mathcal{G}-Ha$ plane for different values of the constant $4c$ appearing in Eq. (48) (solid lines). The dashed lines represent the according $\mathcal{G}=2\,Ha^2/(4c\pi^2)^{3/4}$ condition for the two terms under the radical in (48) to be of the same order of magnitude. Asymptotic slopes to the transition curves obtained by interpolation are also given: they depend little on c and are all around $Ha^{4/5}$.

VI. CONCLUDING REMARKS

We have derived an upper bound for the fractal dimension of the attractor in the case of steady on average forced flow between two electrically insulating parallel plates perpendicular to a strong steady homogeneous magnetic field and over the whole range of nondimensional numbers Ha and Re in 3D or Ha and $\mathcal{G}$ in the quasi-2D case. The derivation of this bound has been achieved by sorting and counting the eigenmodes of a linear operator which is very close to that representing the total dissipation (that is Joule and viscous). Those modes strongly resemble the real turbulent flow in the sense that they exhibit both a wavelength and a boundary layer profile in the vicinity of the walls. This lead us to define some boundaries between different sets of these modes: between quasi-2D and 3D anisotropic sets (with a Joule cone), between sets with and without a Joule cone (strongly/weakly anisotropic) and also between sets with modes exhibiting boundary layer profiles with a single boundary layer thickness of $1/Ha$ and those with boundary layer profiles spanning a broader spectrum of thicknesses.

The apparent similarity between the properties of the least dissipative modes (wavelength, boundary layer thickness) and those of the real flow, as well as between the boundaries separating sets of modes and transitions between turbulent states led us to compare the exact mathematical results obtained in this paper to the heuristics available for turbulent flows. Except for the transition to turbulence in the Hartmann layer, those transitions, length scales, and boundary layer scaling laws exhibit too high exponents for the Reynolds number while the exponents of the Hartmann number are correct. One reason is that the estimate for the inertial terms we start from is known to be an overestimate, whereas the estimation on the linear part of the evolution operator that involves Ha is likely to be optimal. Interestingly, those scaling laws are also identical up to a constant to those derived for the case with periodic boundary conditions,[16] when the flow is far enough from a 2D or quasi-2D state. This underlines that periodic boundary conditions are relevant to the description of 3D wall-bound flows, but not to that of quasi-2D wall bound flows.

The "boundary layer" part of the eigenmodes of the dissipation operator shows a sharp boundary between sets of modes with a single Hartmann layer of thickness $1/Ha$ and sets with multiple boundary layer thicknesses. The law $Ha/Re=$const for this boundary matches the heuristics known for the transition to turbulence of the Hartmann layer in the channel flow configuration on both the exponents of Ha and Re. It should, however, be kept in mind that in channel flows, Re is based on the average velocity whereas our Reynolds number is based on a maximum fluctuating velocity. Together with the finer description of the quasi-2D case and the transition between quasi-2D and 3D turbulence, those "Hartmann layer" properties are the most significant novelty of this work, compared to the previous study with walls.[16]

In the last part of this work, we have addressed the case of quasi-2D MHD turbulence by using the 2D model from Ref. 17. The main advantage of this method is that optimal bounds for the 2D inertial terms are available from the literature. This has allowed us to derive both estimates on the size of small scales as well as a law for the boundary between quasi-2D and 3D sets of modes, expressed as a function of the Grashoff and the Hartmann numbers. The question of knowing whether those results are still optimal, however, remains open. The answer could hopefully come from laboratory experiments, since the presence of Hartmann walls in the present study makes the results derived here directly comparable to experiments.

Lastly, the remarkable similarity between the least dissipative modes derived in this work and the real flow leads to the central question of knowing whether they do represent the flow or not. Answering this question is anything but trivial and the authors believe it might open some interesting perspectives in the study of anisotropic turbulent flows. We shall now finish this discussion by giving some ideas of what it involves. The picture is seemingly "simpler" in hydrodynamic turbulence with periodic boundary conditions where the least dissipative mode are the usual isotropic sequence of Fourier modes used in spectral DNS. Those modes are a basis of $\mathcal{L}_2$ on which any solution including the "real" flow can therefore be expanded. Since it is mathematically proved that the number of vortices in the flow obtained from the Kolmogorov scales by a geometric argument matches the attractor dimension up to a multiplicative constant of the order of 1 (Ref. 8), any optimal upper bound for this dimension gives an exact account of the size of the small scales and tells exactly which finite basis of Fourier modes is required to fully describe the flow at a given Re. The full flow information including nonmodal events and intermittency is, however, not contained in the basis of least dissipative modes itself, but in the time-dependent coefficients of the Fourier expansion, found, for example, by spectral DNS.

Now in the case of MHD turbulence, showing that the number of vortices obtained from the small scales heuristics is also the attractor dimension up to a multiplicative constant, poses no particular difficulty (but goes beyond the scope of this work). In contrast, showing that the least dissipative modes form a basis of $\mathcal{L}_2$ might require an elaborate mathematical proof (in fact, the system of interest is rather the biorthogonal set $\mathcal{B}_{\mathcal{D}_{Ha}}$ made of the canonical system of the dissipation operator $\mathcal{D}_{Ha}$ and that of its adjoint operator,[25,26] but this technical difference, due to the nonorthogonality of the $\mathcal{D}_{Ha}$ operator, is of no influence for our present purpose). Reference 27 has shown that such a system associated to any ordinary differential operator of order n formed a basis of $\mathcal{L}_2$, but this result has yet to be extended to partial differential operators. Let us assume for a moment that this property is valid, as in most of the nonmathematical literature. Then, as in hydrodynamic turbulence, the attractor dimension gives the size of the small scales and indicates which basis of least dissipative modes is required to fully describe the flow for a given values of Ha and Re. Since the least dissipative modes contain not only the two wavelengths $k_\perp$ and κ_z but also the boundary layer thickness, this implies the following:

- If the set of least dissipative modes is 2D, so is the resulting flow.
- If the set of least dissipative modes has a Joule cone, so has the resulting flow.
- If the set of least dissipative modes contains only laminar boundary layer profiles of thickness $1/Ha$, then the Hartmann boundary layers present in the real flows are laminar.

These results, like those for the hydrodynamic case, hold for the modes that achieve any upper bound for the attractor dimension. Now as in the hydrodynamic case, the information about nonmodal events and intermittency is not contained in the basis of least dissipative modes itself, but in the coefficients of the expansion on this basis, which represent the real flow. This implies, for instance, that even when the set of least dissipative modes contains multiple thicknesses, the Hartmann layer can still be laminar, at least intermittently if all the modes with $\delta \neq 0$ have near zero coefficients. The same remark applies to the quasi-2D/3D transition where, for instance, a flow represented by a 3D set of modes can be quasi-2D, at least intermittently.

We are now left with two tasks: mathematicians have to try and prove (or disprove) that $\mathcal{B}_{\mathcal{D}_{Ha}}$ is a basis of $\mathcal{L}_2$. Physicists may not wait for the mathematicians and already perform spectral DNS using these modes in order to calculate the real flow. This may turn out to be very cost effective as the number of modes needed decreases as $1/Ha$, and also because the thin Hartmann layer is finely described by only very few of these modes. The description of this layer traditionally imposes a strong limitation to such numerical calculations as the number of Tchebychev polynomials it requires increases rapidly with Ha. Up to now, this has held cases with $Ha=1000$ out of the reach of DNSs.

ACKNOWLEDGMENT

The authors would like to acknowledge the partial financial support from the Leverhulme Trust, under Grant No. F/09452/A.

APPENDIX: DERIVATION OF A BOUND ON *C*, IN TERMS OF $\mathcal{G}$ AND *Ha*, IN TWO-DIMENSIONAL TURBULENCE

The curl of the governing equation (45) can be written as

$$\frac{\partial}{\partial t}\boldsymbol{\omega} + (\mathbf{u}\cdot\boldsymbol{\nabla})\boldsymbol{\omega} = -Ha\,\boldsymbol{\omega} + \boldsymbol{\nabla}^2\boldsymbol{\omega} + \mathcal{G}\,\boldsymbol{\nabla}\times\mathbf{f}, \tag{A1}$$

where $\boldsymbol{\omega}$ is the vorticity. Multiplying the vorticity equation above by $\boldsymbol{\omega}$ and integrating over the 2D domain yields the enstrophy equation

$$\mathbf{0} = -Ha\int \boldsymbol{\omega}^2 dV + \int \boldsymbol{\omega}\cdot\boldsymbol{\nabla}^2\boldsymbol{\omega} dV + \mathcal{G}\int \boldsymbol{\omega}\cdot\boldsymbol{\nabla}\times\mathbf{f}. \tag{A2}$$

Integrating by part the term in the middle allows us to write the equation under the following form:

$$Ha\int \boldsymbol{\omega}^2\, dV + \int (\boldsymbol{\nabla}^2\mathbf{u})^2\, dV = \mathcal{G}\int \boldsymbol{\omega}\cdot\boldsymbol{\nabla}\times\mathbf{f}\, dV. \tag{A3}$$

Application of Cauchy-Schwartz inequality leads to

$$Ha\int \boldsymbol{\omega}^2 dV + \int (\boldsymbol{\nabla}^2\mathbf{u})^2\, dV \leq \mathcal{G}\sqrt{\int \boldsymbol{\omega}^2\, dV}\sqrt{\int (\boldsymbol{\nabla}\times\mathbf{f})^2\, dV}. \tag{A4}$$

Applying Young's inequality for any positive real number a provides the following expression:

$$Ha\int \boldsymbol{\omega}^2\, dV + \int (\boldsymbol{\nabla}^2\mathbf{u})^2\, dV \leq \frac{\mathcal{G}}{2a}\int \boldsymbol{\omega}^2\, dV + \frac{\mathcal{G}a}{2}\int (\boldsymbol{\nabla}\times\mathbf{f})^2\, dV. \tag{A5}$$

The optimal choice $a = 0.5\mathcal{G}\,Ha^{-1}$ enables us to take advantage of the enstrophy term on the left hand side of (A5), and one can finally obtain the following result:

$$\bar{C} = \sqrt{\int (\boldsymbol{\nabla}^2\mathbf{u})^2 dV} \leq \frac{\mathcal{G}}{2\sqrt{Ha}}\sqrt{\int (\boldsymbol{\nabla}\times\mathbf{f})^2 dV}. \tag{A6}$$

If one restrict ones attention to large-scale forcing, then the dimensionless $\boldsymbol{\nabla}\times\mathbf{f}$ is of order unity, as the dimensionless forcing $\mathbf{f}$ and large scales are of order unity. Hence inequality (A6) becomes

$$\bar{C} = \sqrt{\int (\boldsymbol{\nabla}^2\mathbf{u})^2\, dV} \leqslant \frac{\mathcal{G}}{2\sqrt{Ha}}. \tag{A7}$$

[1] A. Alemany, R. Moreau, P. Sulem, and U. Frish, "Influence of an external magnetic field on homogeneous MHD turbulence," J. Mec. **18**, 277 (1979).
[2] H. M. Hua and W. E. Lykoudis, "Turbulent measurements in magneto-fluid mechanics channel," Nucl. Sci. Eng. **45**, 445 (1974).
[3] J. Sommeria. "Experimental study of the two-dimensional inverse energy cascade in a square box," J. Fluid Mech. **170**, 139 (1986).
[4] A. Pothérat, J. Sommeria, and R. Moreau, "Numerical simulations of an effective two-dimensional model for flows with a transverse magnetic field," J. Fluid Mech. **534**, 115 (2005).
[5] U. Müller and L. Bühler, *Magnetofluiddynamics in Channels and Containers* (Springer, Berlin, 2001).
[6] M. M. Wolf, "L'histoire de la coulée continue première partie," Rev. Metall. **91**, 72 (1994).
[7] K. Ueno and R. Moreau, "Damping rates of magnetohydrodynamic vortices at low magnetic Reynolds number," Phys. Fluids **18**, 025105 (2006).
[8] P. Constantin, C. Foias, O. P. Mannley, and R. Temam, "Determining modes and fractal dimension of turbulent flows," J. Fluid Mech. **150**, 427 (1985).
[9] R. H. Kraichman, "Inertial ranges in two-dimensional turbulence," Phys. Fluids **10**, 1417 (1967).
[10] A. N. Kolmogorov, "Local structure of turbulence in an incompressible fluid at very high Reynolds numbers," Dokl. Akad. Nauk SSSR **30**, 299 (1941).
[11] H. K. Moffatt, "On the suppression of turbulence by a uniform magnetic field," J. Fluid Mech. **28**, 571 (1967).
[12] C. R Doering and J. D. Gibbons, *Applied Analysis of the Navier-Stokes Equation* (Cambridge University Press, Cambridge, 1995).
[13] P. Holmes, J. L. Lumley, and G. Berkooz, *Turbulence, Coherent Structures, Dynamical Systems and Symmetry* (Cambridge University Press, Cambridge, 1996).
[14] P. Constantin, C. Foias, O. P. Mannley, and R. Temam, "Attractors representing turbulent flows," Mem. Am. Math. Soc. **53**, 314 (1985).
[15] P. G. Drazin and W. H. Reid, *Hydrodynamic Stability* (Cambridge University Press, Cambridge, 1995).
[16] A. Pothérat and T. Alboussière, "Small scales and anisotropy in low-Rm MHD turbulence," Phys. Fluids **15**, 3170 (2003).
[17] J. Sommeria and R. Moreau, "Why, how and when MHD turbulence becomes two-dimensional," J. Fluid Mech. **118**, 507 (1982).
[18] R. Moreau, *Magnetohydrodynamics* (Kluwer Academic, Dordrecht, 1990).
[19] T. Alboussière and R. J. Lingwood, "A model for the turbulent Hartmann layer," Phys. Fluids **12**, 1535 (2000).
[20] D. Krasnov, E. Zienicke, O. Zikanov, T. Boeck, and A. Thess, "Numerical study of the instability of the Hartmann layer," J. Fluid Mech. **504**, 183 (2004).
[21] M. Frank, L. Barleon, and U. Mueller, "Visual analysis of two-dimensional magnetohydrodynamics," Phys. Fluids **13**, 2287 (2001).
[22] A. Pothérat, J. Sommeria, and R. Moreau, "An effective two-dimensional model for MHD flows with transverse magnetic field," J. Fluid Mech. **424**, 75 (2000).
[23] P. Constantin, C. Foias, and R. Temam, "On the dimension of the attractors in 2D turbulence," Physica D **30**, 284 (1988).
[24] J. Ohkitani, "Log corrected energy spectrum and attractor dimension in two-dimensional turbulence," Phys. Fluids A **1**, 451 (1989).
[25] M. V. Keldysh, "About eigenvalues and eigenfunctions for some classes of non self-adjoint equations," Dokl. Akad. Nauk SSSR **77**, 11 (1951) (in Russian).
[26] M. V. Keldysh, "On the completeness of eigenfunctions for certain classes of not self-adjoint linear operators," Russ. Math. Surveys **26**, 15 (1971).
[27] V. A. Il'in, "Necessary and sufficient condition for the subsystem of eigenfunctions and associated functions of Keldysh's pencil of ordinary differential operators to form a basis," Dokl. Akad. Nauk SSSR **227**, 796 (1976) (in Russian).